Ayad A. Salih [1]
Asmaa H. Mohammed [2]
Shaymaa H. Aneed [2]
Bushra H. Hussein [1]

[1] *Department of Physics, College of Education for Pure Science / Ibn Al-Haitham, University of Baghdad, Baghdad, IRAQ*
[2] *Department of Physics, College of Science, Al Nahrain University Baghdad, IRAQ*

Fabrication and Optoelectronic Properties of Bismuth Oxide Thin Films Prepared by Thermal Evaporation

This work shows the fabrication of Bi_2O_3/Si heterojunctions for solar cell applications. Bi_2O_3 nanoparticles were deposited on quartz, n- and p-type silicon substrates by thermal evaporation method. The structural and optical characteristics of the prepared Bi_2O_3 thin films were studied. The polycrystalline structure of these thin films was revealed with (111) direction. These Bi_2O_3 thin film has direct energy gap of 2.6 eV. The electrical measurements under dark and light conditions indicate a significant improvement conversion efficiency values for Al/n-Bi_2O_3/n-Si/Al heterojunction. The growth of the depletion layer width with the built-in potential was the cause of the decrease in device capacitance. The photovoltaic measurements were determined and the results showed that the Bi_2O_3/n-Si sample was the best.

Keywords: Thin films; Bismuth oxide; Silicon conductivity type; Solar cells
Received: 19 January 2024; **Revised:** 13 March 2024, **Accepted:** 20 March 2024

1. Introduction

One of the most promising components of a new era in technology and science are nanoparticles (NPs), which are chemical structures with a size between 1 and 100 nm. The market for NPs-based goods is expanding quickly in a number of industries, including biomedical applications, home and garden, electronics and computers, health and fitness, photo cell and photodetector [1-3]. Because of their distinctive and varied physicochemical characteristics, metal oxide nanoparticles have drawn interest from researchers in a variety of fields and one of the important metal oxides that have gained attention recently is Bi_2O_3 [4,5]. Nanostructured Bi_2O_3 thin films have attracted the interest of many researches due to the values of some their characteristics parameters, e.g., available and easy to manufacture, refractive index, photoconductivity, transparency and mechanical strength [3-6]. Also, the energy gap is wide (1.73-3.98eV), it is close to CdS, which is considered a prominent filter for solar cells application [1,6,7]. Although Bi_2O_3-NPs are widely used and purposeful or incidental exposure is rising, nothing is known regarding their toxicity [8]. Different method was used to prepare Bi_2O_3 such as sol-gel [1], pulsed-laser deposition (PLD) [2], green synthesis [4], reactive sputtering [7], spray pyrolysis [9], and magnetron reaction [10]. In order to produce thin films and study their characterization for solar cell applications, bismuth oxide nanoparticles were prepared in this paper using a simple physical method. This is one of the simplest ways to prepare nanoparticles with very perfect crystallinity and deposit them on quartz and other silicon type substrates.

2. Experimental Part

As substrates, test quartz slides with an area of 2x2 cm^2 were used. Alcohol and ultrasonic waves were used to clean them, removing residue and contaminants from their surfaces.

Using a wire-cut machine, square-shaped n & p type silicon samples were created, each measuring 1 cm^2 in area and having resistivities between 1.5 and 4 Ω.cm. For the purpose of removing oxides, the samples were etched using a CP4 solution made up of HNO_3, CH_3COOH and HF in the ratios (3:3:5). After 15 minutes of cleaning with alcohol and ultrasonic waves (using a Berry PUL 125 device), they underwent another 15 minutes of cleaning with water and ultrasonic waves. Ohmic contacts are made on both Bi_2O_3 film and Si substrate by depositing of Al thick films through certain mask using an Edwards thermal evaporation system followed by rapid thermal oxidation. Four-point probe (FPP) technique was used to assess the silicon substrate's resistivity and kind of conductivity. For the TCO's/Si heterojunction, the silicon sample serves as the substrate. The cross-sectional view of Bi_2O_3/Si heterojunction is shown in Fig. (1a).

An Edwards thermal evaporation system was employed to vaporize extreme purity (99.99 %) Bi on quartz slides and Si substrates (n-type and p-type) at room temperature under low pressure (~10^{-6} torr).

Rapid thermal oxidation (RTO) for Bi films was employed to prepare Bi_2O_3 films at different temperature and oxidation time. Figure (1b) depicts

the apparatus used to create the oxide film. To ensure that air (a source of dry oxygen) flowed through it, a quartz cylinder measuring 0.03 m in diameters and having two open ends were employed. Light and heat were radiated by a 650W halogen lamp, and the output power was managed by a variable power supply. Temperature measurements of the sample were made using a k-type thermocouple.

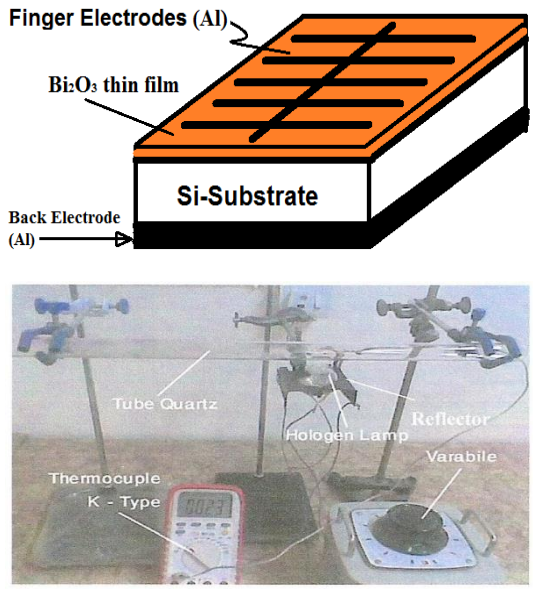

Fig. (1) Cross-sectional view of Bi_2O_3/Si heterojunction (upper), and rapid thermal oxidation (R.T.O) setup (lower)

After being cleaned, the samples were fixed on the quartz tube irradiated by halogen lamp directly. The position of the lamp was fixed to maintain certain temperature, and the distance between the lamp and the tube was 0.5 cm. Thermal oxidation process took place at temperatures between 373 and 973 K, and at different oxidation times in order to obtain the best oxidation of Bi thin films.

3. Results and Discussion

Figure (2) illustrates how to compute the crystalline lattice of inert fixed crystals coordination of single crystal and the preferred trend of polycrystalline crystal using the experimental method of x-ray diffraction (XRD) [11]. XRD pattern of film deposited on the quartz subsurface displays a multicolor construction with a bismuth metal peak at 27.59°, 32.40° and 48.20°, respectively, in the (111), (200) and (116) planes. The conforming d-values have been associated with the JCPDS card, plane (Alpha Order): Bi_2O_3:00-041-1449. The average crystallite size of Bi_2O_3 thin films equal to 29.154 nm was calculated from the Scherrer's formula [12]:

$$C.S = \frac{0.94\,\lambda}{\beta\cos(\theta)} \qquad (1)$$

where $\lambda_{x\text{-ray}}$=1.5406Å, β is (FWHM) of the preferential plane (111)= 0.2932° at 2θ=27.58°

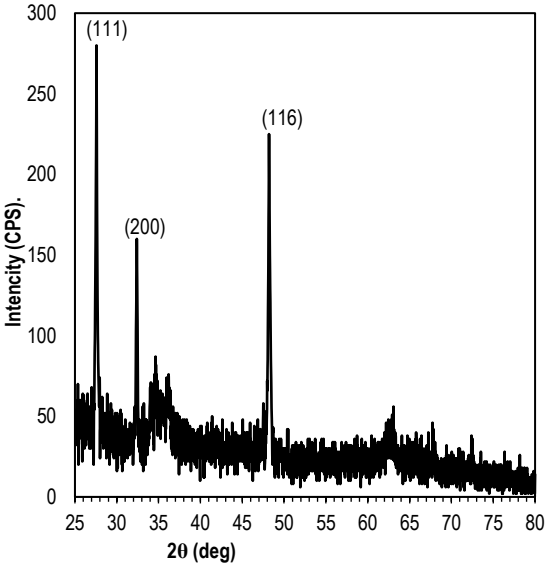

Fig. (2) XRD pattern of the Bi_2O_3 thin film

The SEM microimage of the thin Bi_2O_3 layer on the quartz bottom layer is shown in Fig. (3) at 20 KX magnification. The prepared film has regular distribution granules with uniform and homogeneous surface, thus improving the quality of the prepared films. Additionally, nanostructured grains ranged between 50-90 nm are evenly distributed across the film's surface.

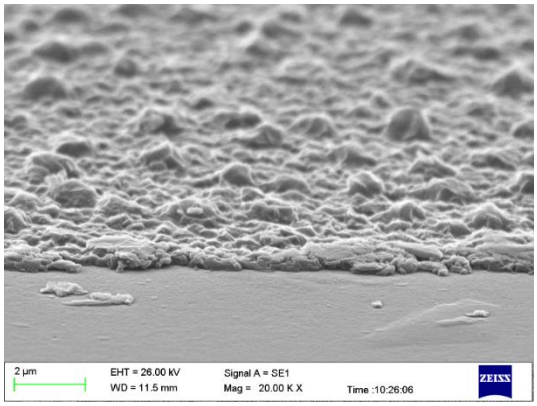

Fig. (3) SEM microimage of the Bi_2O_3 thin film

The UV-visible spectroscopy established the occurrence of nanoparticles by in Fig. (4). The Bi_2O_3 nanoparticles were observed for wavelength scanning between 250-700nm. The characteristic absorption peak of bismuth was detected at 290nm [13]. The energy band gap can be determined using the absorption coefficients with Tauc's equation [14]:

$$(\alpha h\nu) = B(h\nu - E_g)^{n} \qquad (2)$$

where α is the absorption coefficient, ν is the photon frequency, E_g denotes the optical band gap, and B is constant

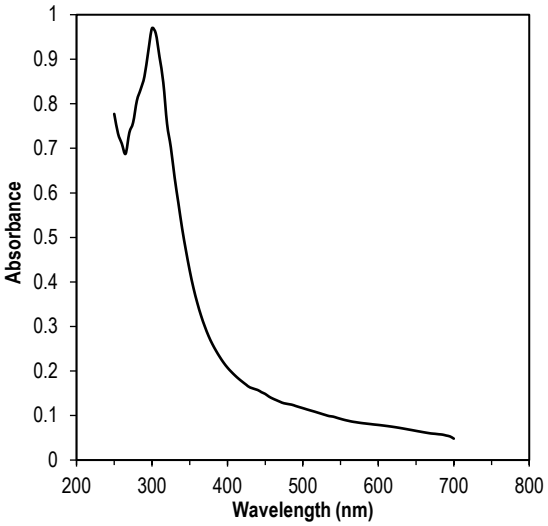

Fig. (4) Absorption spectrum of Bi_2O_3 thin film

The parameter (η) is an index associated with the material's characteristics and determined by the optical transition influencing the absorption process. It dictates the allowed (η = 1/2 and 2) direct and indirect transitions within the electronic band structure. The optical band gap energy (E_g) was obtained from the straight line intersection of the curve as shown in Fig. (5). The band gap is 2.6 eV direct transitions for Bi_2O_3, which is an important characteristic for photovoltaic applications. This value is good agreement with [11].

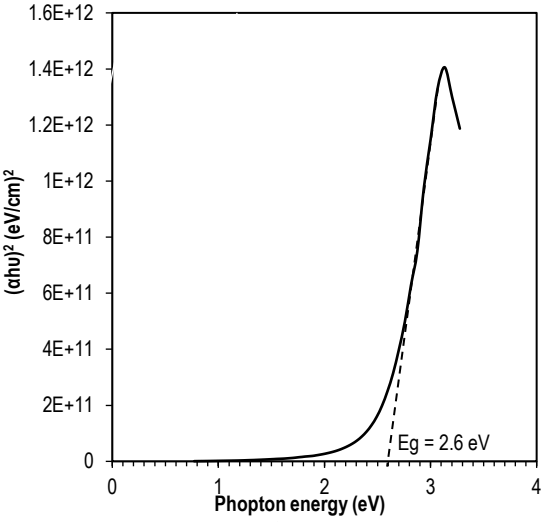

Fig. (5) Variation of $(\alpha h\nu)^2$ with $h\nu$ of Bi_2O_3 thin film

The FTIR absorption spectrum, shown in Fig. (6), was recorded within the range of 400–4000 cm^{-1} to analyze the formation of Bi_2O_3 nanoparticles and identify functional groups. O-H stretching vibrations were evident at 3363~3414 cm^{-1}, while C-O vibrations linked to environmental CO_2 were observed at 2330 cm^{-1}. A peak with 1629 cm^{-1} corresponded to H_2O, and the 542 cm^{-1} peak originated from the metal oxygen (Bi-O) vibration.

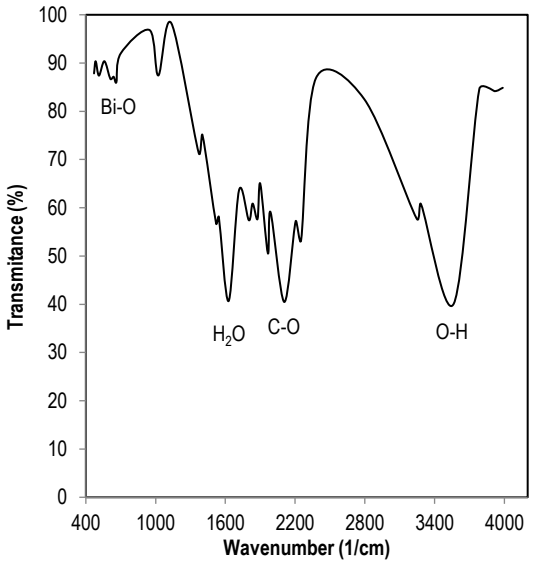

Fig. (6) FTIR spectrum of Bi_2O_3 thin film

Figure (7) displays the outcomes of the electrical measurements (J-V curve) for the devices made from n-Bi_2O_3/SiO_2/n-Si and n-Bi_2O_3/SiO_2/p-Si under ideal conditions at forward and reverse biasing in the dark and illumination. These qualities are crucial for describing the performance of the device and any parameters that depend on it [11]. For two devices operating optimally with reverse bias, the J-V characteristics were given. It has obtained a trace with two distinct sections. The first region is the produced zone, at which the reverse current modestly increases with the related voltage to form pairs of electron-hole at the case of low biasing. Significantly more reverse bias may be seen in the second section. In this instance, diffusion of minority carrier through the connection produced the current. It is evident from the results that n-Bi_2O_3/SiO_2/p-Si produces less current than n-Bi_2O_3/SiO_2/n-Si, that is connected to the substantial junction resistance that lowers leakage current. The improvement in the junction structure is connected to the improvement in the reverse current, which reduces a sum of faults at the semiconductor insulators semiconductor interface of the two junctions. Those flaws are the outcome of strain brought on by mismatched thermal expansion, crystal structure, and lattice parameters. The potential barrier is lowered by the forward voltage in the forward bias, which allows majority carriers to pass it much more easily than they could at zero bias. As a result, the diffusion current exceeds the drift current. The ultimate result is that figure (7) shows how both the n-Bi_2O_3/SiO_2/n-Si and n-Bi_2O_3/SiO_2/p-Si devices behave in terms of J-V characteristics when biased forward. There are two distinct zones; the first one is a recombination current that forms when the generated carrier concentration ($n.p>n_i^2$), or when the produced carrier concentrations are greater than the intrinsic carrier's concentration (n_i), leads to the recombination process.

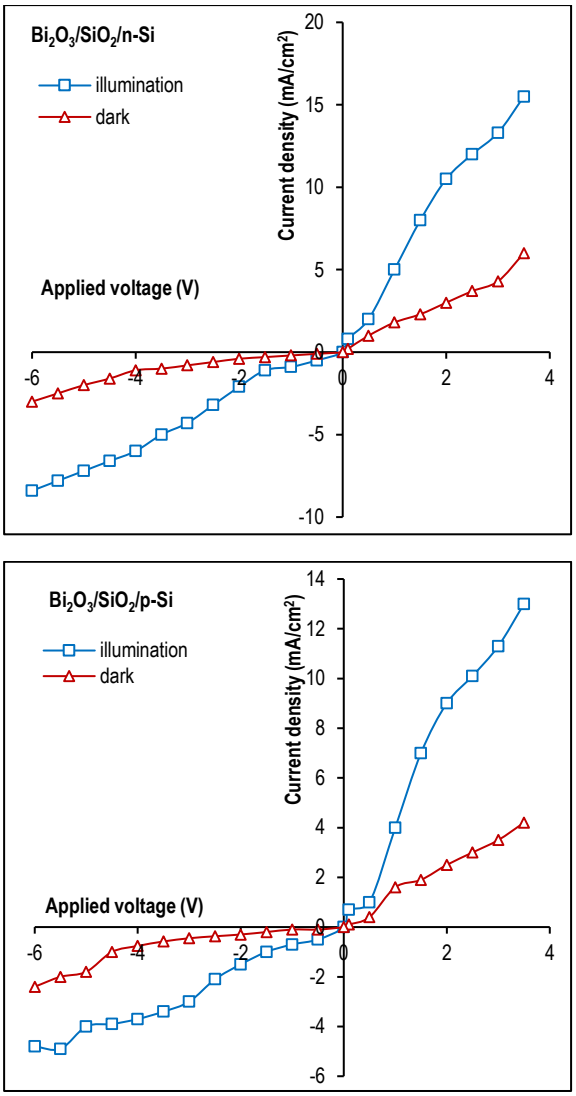

Fig. (7) J-V characteristics for both MIS devices under forward and reverse bias

Depending on the series resistance, second zone when high voltages indicated the diffusion and bending regions, which in the case of MIS characterized the tunneling regions. It is clear from a contrast of the results of the two devices created under ideal conditions that the value of the current enhanced for n-Bi_2O_3/SiO_2/n-Si because a reduction in resistivity of n-type silicon leads to a growth in the electron concentrations. Because of the thicker SiO_2 layer used in the n-Bi_2O_3/SiO_2/n-Si device, this results in a decrease the holes concentrations, hence a corresponding fall in I_s. Being able to determine several factors, including built-in potential (V_{bi}), device capacitance (C_o), and device kind, makes it one of the most crucial measures. The measurements for C-V and $1/C^2$-V for each device are shown in Fig. (8).

The findings indicate that the devices capacitances are inverse related to the bias voltage. The growth of the depletion layers (W) with the built-in potential (V_{bi}) caused the device capacitance to decrease with the related bias voltage. The capacitance of depletion layers is increased with increasing the applied voltage. The action of charge transfer from donor to the acceptor zone, was discovered to be abrupt is accurately indicated with this, and is further verified by the fact that the relationship between $1/C^2$ and reverse bias are straight lines. Given that band bending occurs mainly on the silicon side, the small-single capacitance-volt characteristic can be used to measure the potential barrier for the junction. The point where the curve intersects the x-axis corresponds to the diffusion potential of silicon as shown in table (1), and its values are anticipated to be solely dependent on the Fermi level within the conduction band at elevated carrier concentration. Donor concentration (N_D) is determined by the straight line's slope, and its value closely matches the silicon substrate's well-known resistivity.

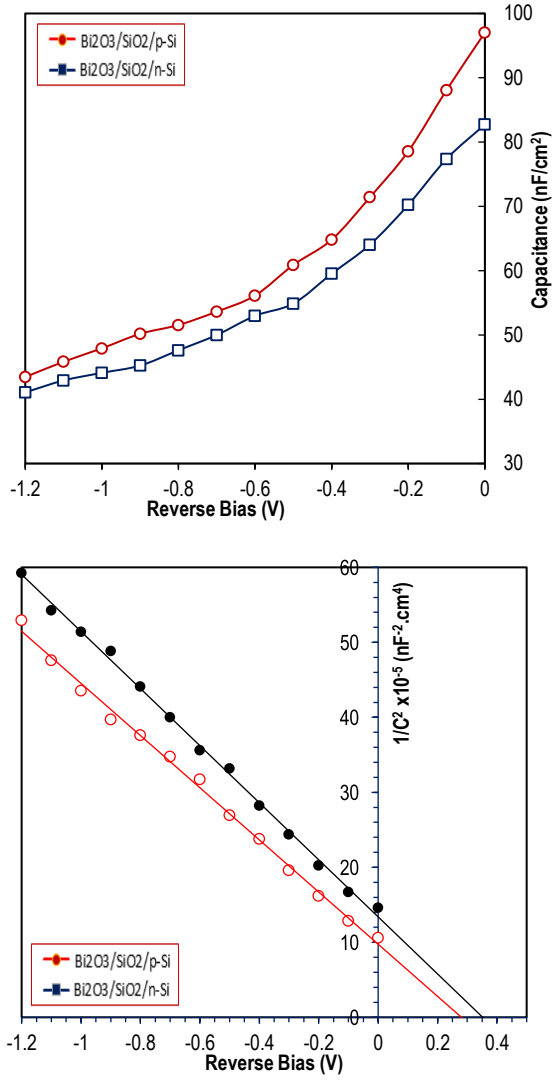

Fig. (8) The relationship between junction capacitance and applied voltage for both MIS devices, at f=100 kHz

Table (1) Values of C-V diagram for Bi_2O_3/SiO_2/Si heterojunctions

Si substrate type	V_{bi} (V)	C_o (nf/cm²)	$W=\varepsilon_s/C_o$ (μm)	$N_D x10^{+15}$ (cm^{-3})
n-Bi_2O_3/SiO_2/ p-Si	0.27	100.00	7.303	2.37978
n-Bi_2O_3/SiO_2/ n-Si	0.35	91.29	7.999	2.39564

In Fig. (9), the relationship between the incidence photons power of the halogen lamp and the short circuit current (I_{SC}) and open circuit voltage (V_{OC}) for both devices is depicted. According to the results, there is a linear relationship between I_{SC} and V_{OC}, by the photo powers incident having a maximum value beyond with both values for the two devices tending for becoming saturated and constant. This is brought on by the complete separations of the electron-hole pairs produced by the photons. It is evident that there is a significant disparity between the values of the obtained results. The increased performance of the n-Bi_2O_3/SiO_2/n-Si device was due to widening of the depletion layer (*W*) caused by addition of the interfacial thickness (SiO_2), which results in large areas for the separation of electron-hole pair and hence a significant photocurrent.

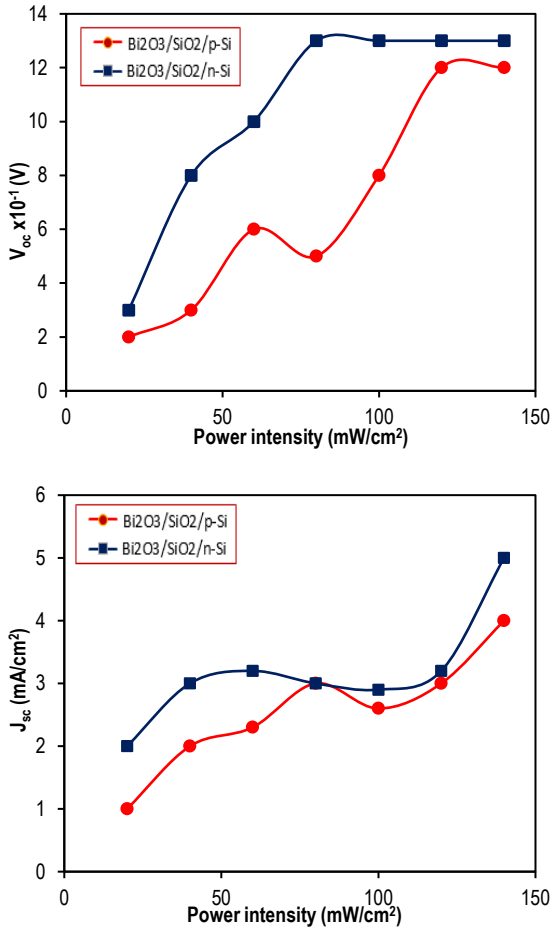

Fig. (9) Variation of open-circuit voltage and short-circuit current density with incident power intensity for both MIS devices

Figure (10) represents J-V characteristics of both n-Bi_2O_3/SiO_2/n-Si and n-Bi_2O_3/SiO_2/p-Si solar cells, the short-circuit current value (I_{SC}) determined at V=0, while the open-circuit voltage (V_{OC}) was determined at I=0, as shown in table (2), where the value of fill factor (F.F) and the photovoltaic conversion solar cell efficiency (η) are calculated from the following equations [14]:

$$\eta = \frac{P_m}{P_{in}} \times 100\% = \frac{I_m \cdot V_m}{P_{in}} \times 100\% \quad (3)$$

$$\text{F.F.} = \frac{J_m \cdot V_m}{J_{sc} \cdot V_{oc}} \quad (4)$$

Table (2) Electrical parameters for (a) n-Bi_2O_3/SiO_2/n-Si and (b) n-Bi_2O_3/SiO_2/p-Si heterojunction solar cells

Si substrate type	V_{oc} (V)	J_{sc} (mA/cm²)	V_{max}, V_m (V)	J_{max}, J_m (mA/cm²)	F.F	η %
(a)	1.3	2.9	0.84	1.9	0.423	1.6
(b)	0.8	2.6	0.52	1.6	0.400	0.83

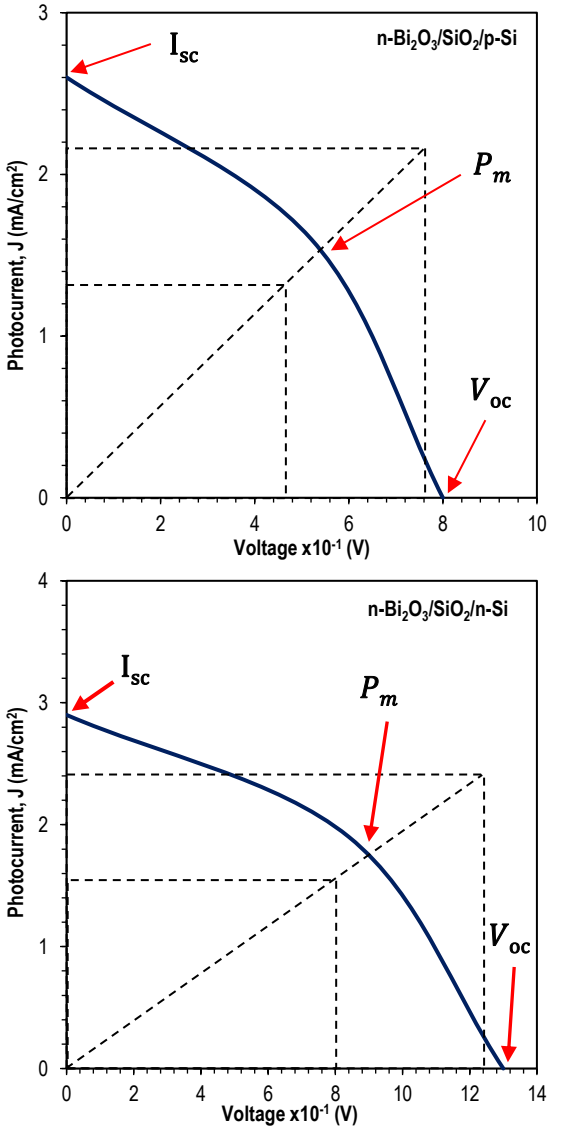

Fig. (10) J-V curves of n-Bi_2O_3/SiO_2/p-Si and n-Bi_2O_3/SiO_2/n-Si heterojunction solar cells

4. Conclusions

The Bi_2O_3 thin films prepared in this work were polycrystalline with grain size of 15-29nm and uniform surface. The direct optical energy gap was found to be 2.6 eV. The photovoltaic outcome for the n-Bi_2O_3/(n,p)Si heterojunction was found to be a linear relationship between I_{SC} and V_{OC}. The I-V and C-V measurements of the heterojunctions depends on the silicon substrate type. The efficiency of solar cell fabricated on n-type silicon substrate is higher than that fabricated on p-type silicon substrate due to less light-induced degradation.

References

[1] W. He et al., "Thin bismuth oxide films prepared through the sol–gel method", *Mater. Lett.*, 61(19) (2007) 4100-4102.

[2] E.T. Salim et al., "Optical properties of Cauliflower like Bi_2O_3 nanostructures by reactive pulsed laser deposition (PLD) technique", *Sol. Ener.*, 107 (2014) 523-529.

[3] E. Hashemi, R. Poursalehi and H. Delavari, "Formation mechanisms, structural and optical properties of Bi/Bi_2O_3 One dimensional nanostructures prepared via oriented aggregation of bismuth based nanoparticles synthesized by DC arc discharge in water", *Mater. Sci. Semicond. Process.*, 89 (2019) 51-58.

[4] N. Motakef-Kazemi and M. Yaqoubi, "Green Synthesis and Characterization of Bismuth Oxide Nanoparticle Using Mentha Pulegium Extract", *Iranian J. Pharmaceut. Res.*, 19(2) (2020) 70-79.

[5] C.M. Hincapie et al., "Physical-Chemical Properties of Bismuth and Bismuth Oxides: synthesis, characterization and applications", *DYNA*, 176 (2012) 139-148.

[6] R.A. Ismail, "Fabrication and Characteristics Study of n-Bi_2O_3/n-Si Heterojunction", *J. Semicond. Technol. Sci.*, 6(2) (2006) 119-123.

[7] H.T. Fan et al., "δ-Bi_2O_3 thin films prepared by reactive sputtering Fabrication and characterization", *Thin Solid Films*, 513 (2006) 142–147.

[8] E. Öztaş et al., "Bismuth oxide nanoparticles induced oxidative stress-related inflammation in SH-SY5Y cell line", *Istanbul J. Pharm.*, 49(3) (2019) 173-179.

[9] T.P. Gujar, V.R. Shinde and C.D. Lokhande, "Spray pyrolysis bismuth oxide thin films and their characterization", *Mater. Res. Bull.*, 41 (2006) 1558-1564.

[10] J. Morasch et al., "Reactively magnetron sputtered Bi_2O_3 thin films: Analysis of structure, optoelectronic, interface, and photovoltaic properties", *phys. stat. sol. (a) Appl. Mater.*, 211(1) (2014) 342.

[11] B.K. Hasson and N.I. Najm, "The Influence of Aluminum Doping on Structural and Optical Properties of (Bi_2O_3) Thin Films", *Ibn Al-Haitham J. Pure Appl. Sci.*, 29(2) (2016) 387-396.

[12] B.D. Dullity, **"Elements of X-Ray Diffraction"**, Addison-Wesley Publishing Co., Inc. (USA, 1956), p. 99.

[13] L. Leontie et al., "Structural and Optical Characteristics of Bismuth Oxide Thin Films", *Surf. Sci.*, 507 (2002) 480-485.

[14] S.M. Sze, **"Physics of Semiconductor Devices"**, 3rd ed., John-Wiley & Sons, Inc. (Canada, 2007).

